


Article

# Synthesis, Reactivity Studies, and Cytotoxicity of Two *trans*-Iodidoplatinum(II) Complexes. Does Photoactivation Work?

Leticia Cubo <sup>1</sup>, Thalia Parro <sup>1</sup>, Amancio Carnero <sup>2</sup>, Luca Salassa <sup>3</sup>, Ana I. Matesanz <sup>1</sup> and Adoracion G. Quiroga <sup>1,\*</sup> 

<sup>1</sup> Departamento de Química Inorgánica, Universidad Autónoma de Madrid, 28049-Madrid, Spain; leticia.cubo@uam.es (L.C.); thalia.pd20@gmail.com (T.P.); ana.matesanz@uam.es (A.I.M.)

<sup>2</sup> IBIS, Campus Hospital Universitario Virgen del Rocío, 41013-Sevilla, Spain; acarnero@us.es

<sup>3</sup> Donostia International Physics Center, 20018-Donostia, Spain; lsalassa@dipc.org

\* Correspondence: adoracion.gomez@uam.es; Tel.: +34-914974050

Received: 19 October 2018; Accepted: 23 November 2018; Published: 3 December 2018



**Abstract:** *trans*-Platinum complexes have been the landmark in unconventional drugs prompting the development of innovative structures that might exhibit chemical and biological profiles different to cisplatin. Iodido complexes signaled a new turning point in the platinum drug design field when their cytotoxicity was reevaluated and reported. In this new study, we have synthesized and evaluated diiodoplatinum complexes *trans*-[PtI<sub>2</sub>(amine)(pyridine)] bearing aliphatic amines (isopropylamine and methylamine) and pyridines in *trans* configuration. X-ray diffraction data support the structural characterization. Their cytotoxicity has been evaluated in tumor cell lines such as SAOS-2, A375, T-47D, and HCT116. Moreover, we report their solution behavior and reactivity with biological models. Ultraviolet-a (UVA) irradiation induces an increase in their reactivity towards model nucleobase 5'-GMP in early stages, and promotes the release of the pyridine ligand (spectator ligand) at longer reaction times. Density Functional calculations have been performed and the results are compared with our previous studies with other iodido derivatives.

**Keywords:** platinum iodido complexes; cytotoxicity; photoactivation

## 1. Introduction

Antitumor platinum drug design has been and still is a major project in metallodrug research. The latest reviews and the large number of contributions therein identify new complex designs to face the known side effect problems of these antitumor drugs [1]. One of the latest contributions to this field has been the results that we published when studying the impact of the leaving group in the reactivity and cytotoxicity of the iodido complexes [2,3]. Looking for a new design, our group of researchers reevaluated *cis* platinum iodido complexes; their reactivity turned out to be quite unexpected versus sulfur donor biomolecules [4]. Our studies proved that the iodido groups stayed in the adducts formed in the reaction with the protein cytochrome c or lysozyme while the aliphatic amines acted as leaving groups [5]. This peculiar reactivity was not detected versus DNA, with which they showed classical reactivity cisplatin like.

Following these results, we extended our studies to include the reactivity of *trans* diiodido diamine platinum(II) with different aliphatic amines versus some selected models of biomolecules [6]. These reactivity studies revealed a very similar profile for the *cis* and *trans* complexes upon binding to model nucleobases (DNA). The adduct formation occurs with retention of the amine spectator ligands. Additionally, *trans*-type complexes manifested a lower propensity to form adducts with peptide and a more classical reactivity, the iodido ligands release upon protein binding. Moreover,

these last *trans* series seemed to be affected by the size of the amine ligands showing differences in their reactivity versus S-donor models and in their cytotoxicity [6]. The reconsideration of these iodido derivatives have shown a great impact in the field, and the trend and behavior of these complexes is being reevaluated [7].

Within the design of novel metallodrugs, the use of activation therapies such as the use of UVA light offers a wide fan of possibilities for metallic complexes such as activation of reactivity [8], change in conformation [9], heterobimetallic complexes with PDT ligands [10] and singlet oxygen producing complexes [11]. Photochemical studies on a selected number of *trans* iodido complexes initially showed that irradiation induces a faster reaction with CT DNA and a higher amount of Pt bound to DNA. These complexes also reacted faster with 5'-GMP under irradiation and even showed noticeable improvements in their cytotoxicity when treatment was combined with UVA light [12]. These results support the idea that UVA light could be used to increase the activity of the diiodido platinum complexes, and might even make it more selective, in a similar way than those observed for chlorido derivatives [8].

Within this frame, we have looked at the role of the spectator ligand within the iodido complex structures and replaced one of the aliphatic amines with an aromatic planar amine, widely used in the *trans* type of complexes with highly satisfying results [13]. In particular, we prepared two *trans* configured iodido-platinum complexes with a pyridine and isopropylamine/methylamine ligands. X-ray structure studies of both complexes complete the structural characterization. The cytotoxicity was evaluated and the possible mechanism investigated, looking for a possible photochemical activation. The interaction studies of these new complexes with a representative model biomolecules such as: model nucleobase 5'-GMP and *N*-Methylimidazol (MeIm) have been performed and photochemical studies on such interaction analyzed and discussed together with the DFT calculations.

## 2. Results

### 2.1. Synthesis and Characterization

The *trans*-[PtI<sub>2</sub>(amine)(pyridine)] complexes were prepared according to published procedures with slight variations, using the *cis*-[PtI<sub>2</sub>(amine)<sub>2</sub>] complexes with the corresponding aliphatic amine: isopropylamine or methylamine as the starting material [6]. The reaction was carried out in water with an excess of pyridine and without isolating the tetraamine species, giving the desired *trans* complexes by slow evaporation of the solvent at high temperature.

The structure and numbering of the complexes are depicted in Figure 1. Their characterization performed by usual techniques is nicely in agreement with the proposed structure and detailed data have been collected in the experimental section.

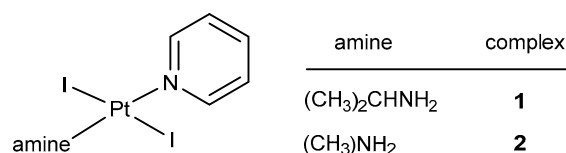


**Figure 1.** Structure and numbering of the complexes studied in this manuscript.

The molecular structure of complexes 1 and 2 are shown in Figure 2. Crystal data are listed in Table S1. Selected bond lengths and angles are shown in Table 1. The platinum(II) atom has a square planar coordination geometry and is coordinated to two nitrogen atoms of the methylamine or isopropylamine and pyridine ligands and two iodido ligands in *trans*-arrangement.

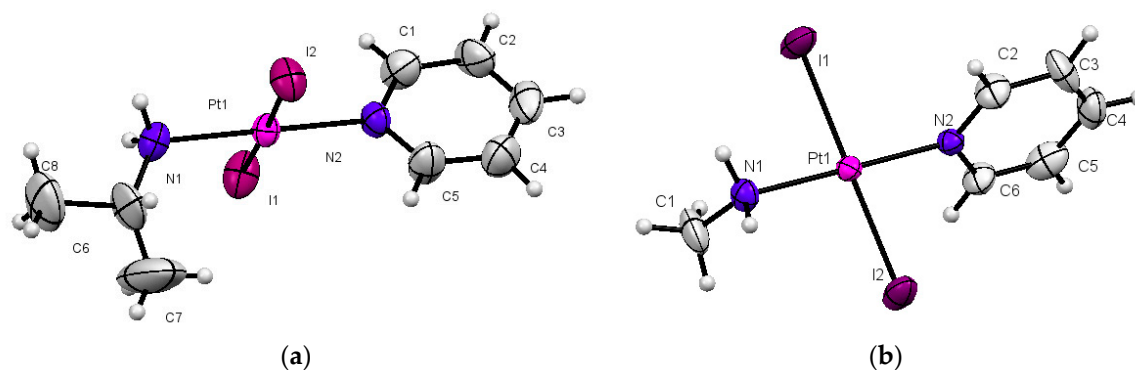


**Figure 2.** Molecular views: (a) complex 1 (b) complex 2.

**Table 1.** Selected distances (Å) and angles (°) in complexes 1 and 2.

Distances	Complex 1	Complex 2
Pt–I1	2.5962(9)	2.5906(11)
Pt–I2	2.5920(8)	2.59861(19)
Pt–N1	2.050(9)	2.077(13)
Pt–N2	2.014(8)	2.025(13)
Angles	Complex 1	Complex 2
N2–Pt–N1	179.24(4)	179.3(5)
N1–Pt–I1	90.1(3)	90.2(4)
N1–Pt–I2	90.0(3)	89.1(4)
N2–Pt–I1	89.7(3)	90.1(4)
N2–Pt–I2	90.02(3)	90.6(4)
I1–Pt–I2	179.05(3)	177.24(4)

## 2.2. Cytotoxicity of *trans*-[PtI<sub>2</sub>(amine)(py)] Complexes

The cytotoxicity of complexes 1 and 2 was determined in comparison to cisplatin. The cancer cell lines selected for this study are SAOS-2 (human osteosarcoma), A375 (melanoma), T-47D (breast carcinoma), HCT116++ (human colon carcinoma with the presence of p53) and HCT116– (human colon carcinoma in the absence of p53). The IC<sub>50</sub> and standard deviation values for complexes 1 and 2 are shown in Table 2.

**Table 2.** IC<sub>50</sub> values for complexes 1 and 2 and cisplatin in five cancer cell lines. Data were collected after 96 h of exposure to the drugs. Standard deviation is shown in brackets.

Cell line	Complex 1	Complex 2	Cisplatin
SAOS-2	32.9 (22.6) *	53.7(15.8)	5.9(1.5)
A375	18.9(3.4)	27.9(5.1)	9.2(1.7)
T-47D	30.9(5.6)	45.0(2.5)	10.2(3.4)
HCT116++	18.1(3.6)	29.8(4.4)	8.3(2.7)
HCT116– –	56.4(10.3)	63.4(17.3)	62.2(14.3)

\* This value could be an overestimated number, because of the high standard deviation.

## 2.3. Reactivity of *trans*-[PtI<sub>2</sub>(amine)(py)] Complexes with 5'-GMP and MeIm

One of the main cellular targets of metallodrugs is DNA [14,15]. There are many techniques to study the interaction with DNA, since our objective in this section is to compare the reactivity of these compounds with the data available in the references, we have used a small model of DNA, such as 5'-GMP to carry out the experiments. This model has proved to be an excellent approach in many systems by monitoring the changes at its H8 signal by <sup>1</sup>H NMR [16,17].

Thus, the study on the reactivity of complexes **1** and **2** with the model nucleobase 5'-GMP was carried out. The complexes under investigation were incubated at a molar ratio of complex: 5'-GMP of 1:2 as described in the experimental section and the reactivity toward this nucleobase was monitored by NMR spectroscopy. The  $^1\text{H}$  NMR spectra of the interaction of complex **1** with 5'-GMP monitored in a mixture of acetone- $d_6$  and  $\text{D}_2\text{O}$  (ratio 2:1) from 1 h to 7 h are shown in Figure 3. When following the changes at the H8 peak signal of 5'-GMP, a new signal arises at 9.1 ppm that is assignable to a H8 nucleotide adduct and the intensity increases during the first 3 h of reaction while the H8-signal of the free nucleotide decreases. At longer reaction times, the first monoadduct intensity does not increase and simultaneously, a new adduct is detected at 8.2 ppm. The monitoring of the reaction provides evidence for the presence of 5'-GMP adducts in the sample (label S at Figure 3 and Figure S1). The reaction of the *trans* complex **2** with 5'-GMP was also studied and the results are similar to the reactivity described for complex **1**. However, the reactivity of compound **2** seems to be slower since the signals assigned to the adduct species are weaker in complex **2** than for complex **1** after 3 h of reaction (Figure S2). Furthermore, a smaller amount of the model nucleotide adducts are detected for complex **2** over longer periods of time.

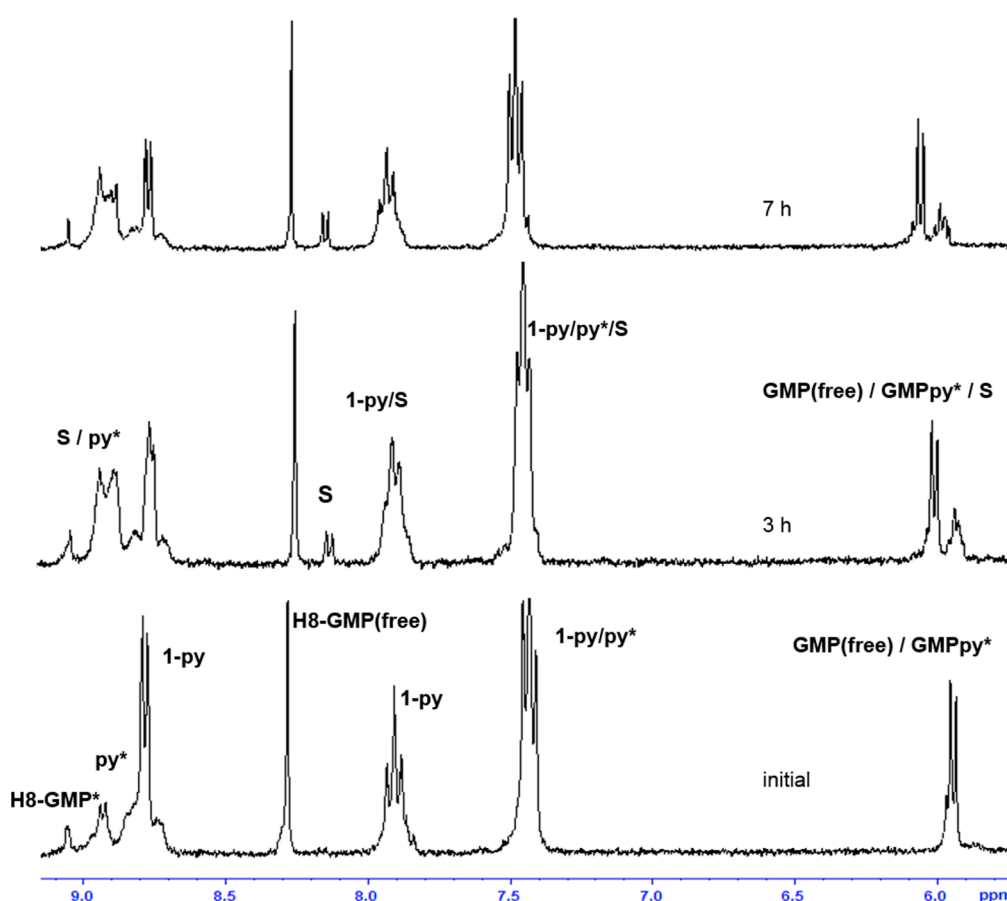


**Figure 3.** Progress of the reaction between complex **1** and 5'-GMP at 37 °C monitored by  $^1\text{H}$  NMR (acetone- $d_6$  and  $\text{D}_2\text{O}$  in a ratio 2:1) showing changes in the aromatic area. Labels: GMP(free), free 5'-GMP; H8-GMP\*: H8-5'-GMP coordinated adduct signal; 1-py, pyridine ligand signals of complex **1**; py\*, adduct pyridine signal, and S: speciation.

When similar experiments were repeated under irradiation, the reactivity of complex **1** with 5'-GMP showed some important differences compared to the non-irradiated sample. In the first hour of irradiation, the reported monoadduct is formed in a higher amount (integrals shows a higher formation), but after 1 h the spectra shows a new signal at 8.6 ppm (Figure 4) corresponding to free pyridine and its intensity increases along the time. Moreover, we can clearly observe new species in

the high-field region of the spectra and there are also signals corresponding to the isopropylamine group that appear to split into several sets.

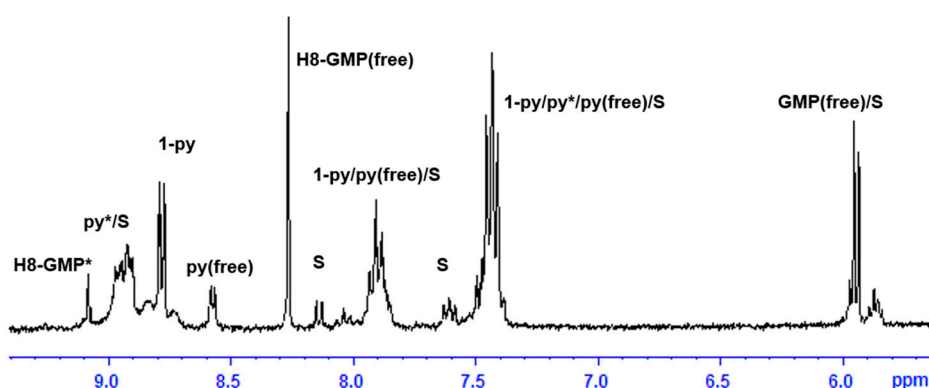


**Figure 4.**  $^1\text{H}$  NMR spectrum of the reaction between complex 1 and 5'-GMP (acetone- $d_6$  and  $\text{D}_2\text{O}$  in a ratio 2:1) showing changes in the aromatic and aliphatic area after 1 h under irradiation at 37 °C. Labels: GMP(free), free 5'-GMP; H8-GMP\*: H8-5'-GMP coordinated adduct signal; 2-py, pyridine ligand signals of complex 2; py\*, adduct pyridine signal, and S: speciation.

In addition, we extended our NMR study of the complexes' coordination to the heterocyclic ligand *N*-methylimidazole, MeIm. It has been reported that this model can provide information about the possibilities of a complex to bind into a lopsided configuration like those presented by biological molecules such as proteins or DNA [18]. Moreover, its structure is different to 5'-GMP (already used) but similar to those presented by proteins at, for example, histidine's sites. We monitored the reactivity with this model at 37 °C (Figure 5a) and detected monoadduct species formation within the first hour, becoming almost a major product only after 3 h. The speciation is clearly formed quickly and the starting material has fully reacted after 7 h. The photoactivation of the sample (Figure 5b) enhances the reactivity but more importantly, produces the release of the pyridine ligand like in its reaction with 5'-GMP.

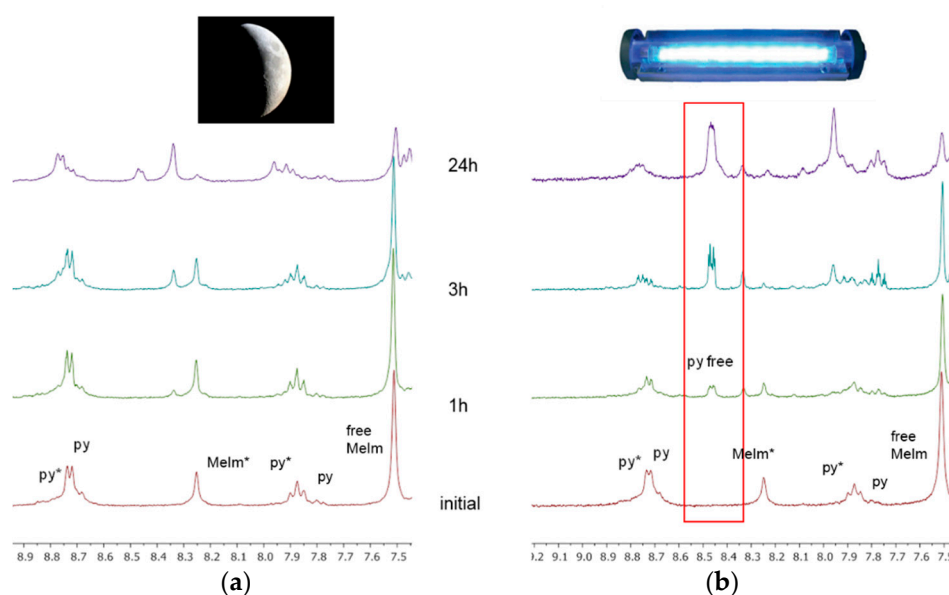


**Figure 5.** Progress of the reaction between complex 1 and MeIm monitored by  $^1\text{H}$  NMR (acetone- $d_6$  and  $\text{D}_2\text{O}$  in a ratio 2:1) showing changes in the aromatic area. Labels: py, pyridine ligand complex 1; py\*, pyridine signal adducts, MeIm\*, *N*-Methylimidazol signal adducts, free MeIm, free *N*-Methylimidazol. (a) reaction at 37 °C and (b) reaction at 37 °C and irradiating.

#### 2.4. DFT Calculations

For a better understanding of the photochemistry of these *trans*-iodido platinum(II) complexes, we performed a set of Density Functional Theory (DFT) and time-dependent DFT (TD-DFT) calculations on complexes **1** and **2** and their 9-EtG adducts. The DNA basis mimic, 9-EtG, was used instead of 5'-GMP to ease the computational calculations. After geometry optimization (Table S2a–d), we analyzed the single-singlet transitions on the complexes and gauged their excited-state chemistry (Tables S3 and S4). Consistently with experimental results, the parent complexes **1** and **2** display electronic transition that are mostly dissociative towards the iodido ligands (Table S3). The calculated absorption spectrum of the mono 9-EtG adducts of the two complexes displays a band at ca. 350 nm, which can be excited under UVA excitation (Table S5). Both mono and bis 9-EtG adducts present a dissociative transition towards the four ligands, as shown in the electron difference density maps (EDDMs, Table S6). As an example, Figure 6 (and Table S7) reports two EDDMs for complexes **1** and **2** corresponding to the calculated lowest-energy electronic transition in which the antibonding orbitals LUMO+4 and 5 have significant contributions. According to this scenario, the 9-EtG adducts are more likely to prompt the release of a pyridine under light irradiation compared to the parent **1** and **2**. A summary of the most relevant bond distances for **1** and **2** and their 9Et-G derivatives are reported in Table S8.

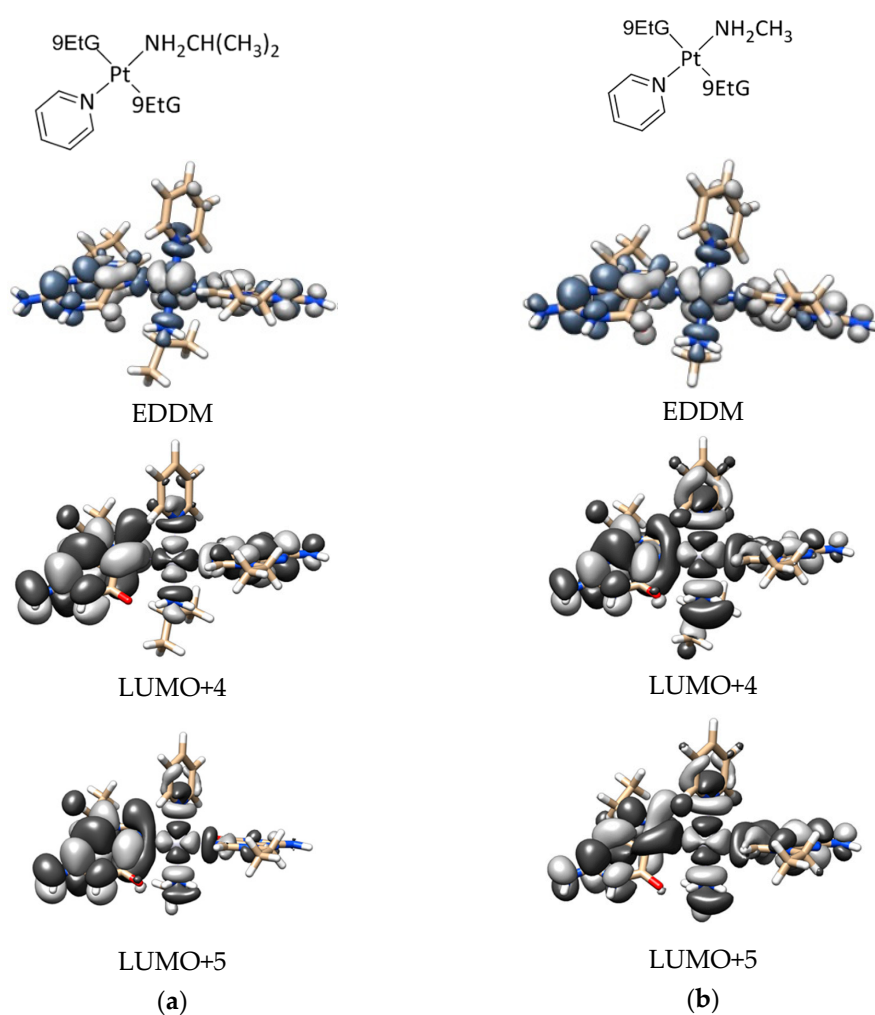


**Figure 6.** Selected electron difference density maps (EDDMs, transition 1, Table S7) and corresponding LUMOs for the bis 9-EtG adducts of complexes **1** (a) and **2** (b) in water at the CAM-B3LYP/LANL08/6-31G\*\* level. In the EDDMs (top), gray indicates a decrease in electron density, while blue–gray indicates an increase.



### 3. Discussion

The complexes were designed based on the positive results achieved with previous complexes of nonconventional structure and using iodidos, aliphatic amines, and pyridine as ligands. The synthesis was performed following our published procedure, although the final yields obtained for complexes **1** and **2** are lower than usual. Many attempts for varying concentrations, temperature or longer reaction time did not improve the results. The characterization by usual techniques was in accordance with the X-Ray study and allowed for a detailed knowledge of the structural features. The mentioned structures are compared with those of published Pt complexes with aliphatic amines, iodide, and pyridine ligands. The Pt–N (aliphatic amine) [19,20], Pt–I [21,22] and Pt–N (pyridine) [23,24] distances fall in the typical ranges. The interactions between the methyl groups and the iodido ligands result in significant strain in the complexes. This is reflected in the deviation of the Pt–N–C angles ( $116^\circ$ ) from the ideal tetrahedral values ( $109^\circ$ ). Cytotoxicity was evaluated versus SAOS-2 human osteosarcoma, A375 melanoma, T-47D breast cancer, SF-268 glioblastoma, NCI-H460 lung cancer and colorectal carcinoma HCT116, and matched p53-deficient HCT116 (-/-) cell lines. The antiproliferative effects are found to be moderate, with  $IC_{50}$  values generally being in the micromolar range and the differences between the cytotoxic potencies of complexes **1** and **2** are comparatively small. Substitution of one aliphatic amine by pyridine seems to decrease cytotoxic potency; the steric demand could be responsible for these poor specific antitumor effects. We believe that irradiation of the complexes will produce the enhancement of the antitumoral activity, as discussed in the following results.

- The interaction of these complexes with 5'-GMP shows the formation of the expected DNA adduct after hydrolysis of the iodido complexes as reported for similar compounds with no release of the spectator ligands.
- However, once we irradiate the samples, we can only observe a promotion of the reactivity in the first hour, and then the release of the pyridine ligand becomes clear at longer reaction times under irradiation.
- This release of the spectator ligand, enhanced by irradiation, has not been observed studying *trans* isomers with iodido ligands versus DNA [6], but only with *cis* isomers and versus proteins [5]. In addition, when the results of the interaction of compounds **1** and **2** with MeIm are evaluated, they are very similar to the results obtained with DNA.
- Our interpretation of the data is that after irradiation, the reactivity of complexes **1** and **2** is enhanced, forming active species. However, at longer reaction times, the compounds lose the pyridine, affording new adducts and species that are more similar to those reported from the cytotoxic compounds than their original aqua species/adducts.
- DFT calculations justify the quicker formation of the bis/monoadduct species (Figure 6) along the first hour, but once the irradiation applies for longer periods of time, the pyridine is released and the compound is no longer the structure proposed but similar to those bearing only aliphatic amines [12].

The potential photoactivation of these poor pharmacological complexes is apparently not a simple mechanism. In the short term the irradiation will afford the DNA adducts but the most effective photoactivation will take place in the long term, as the species will be the same as the most active iodido series reported previously (Figure 7).

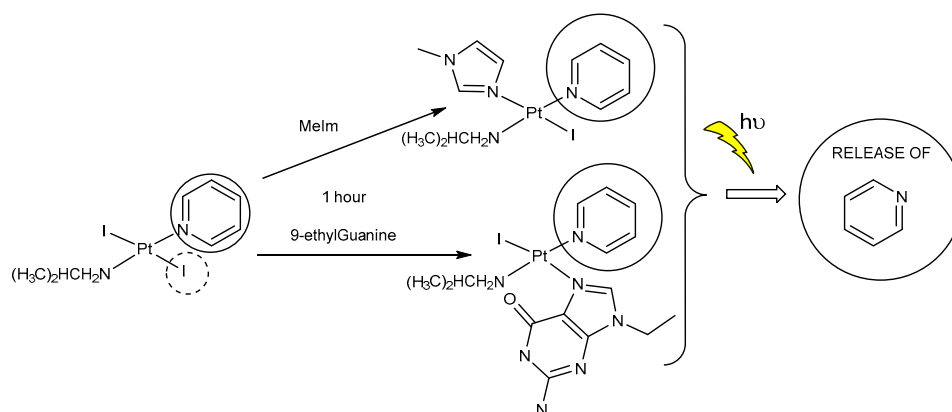


Figure 7. Reactivity versus 9-EtG and MeIm proposed in the discussion.

#### 4. Materials and Methods

Complexes  $cis\text{-PtI}_2(\text{amine})_2$  (where amine = isopropylamine or methylamine) were synthesized as described in the previous communications based on reported procedures [12]. Characterization was in agreement with our previous data. Chemical starting materials;  $\text{K}_2\text{PtCl}_4$ , amines, pyridine and biological molecules—were purchased from VWR (Madrid, Spain).

##### 4.1. Method for the Synthesis of $trans\text{-[PtI}_2(\text{amine})(\text{pyridine})]$

We followed published methods with slight variations, briefly: 500 mg of  $cis\text{-PtI}_2(\text{amine})_2$  (where amine is ipa for **1** and ma for **2**) and 20 equivalents of pyridine were mixed together in 30 mL of water and heated at reflux temperature for 3–6 h. The suspension turned to an almost clear solution that was filtered over celite. The resulting solution was concentrated very slowly at high temperature (100 °C) until the detection of an orange solid, which was allowed to stand overnight at 4 °C until complete precipitation. Then, the solid was filtered off, washed with warm water, and vacuum dried overnight at 60 °C in a drying oven. Afterwards, recrystallization in chloroform/ether was required. Single crystals were achieved by slow evaporation of a chloroform solution.

$trans\text{-[PtI}_2(\text{ipa})(\text{py})]$  **1** (orange solid). Yield: 18%. Elemental analysis found, C, 16.23; H, 2.44; N, 4.63;  $\text{C}_6\text{H}_{10}\text{I}_2\text{N}_2\text{Pt}$  requires C, 16.37; H, 2.40; N, 4.77. NMR (acetone- $d_6$ ):  $\delta$  (1H): 1.33 (d,  $J = 6.46$  Hz, 6H, 2 $\text{CH}_3\text{-ipa}$ ), 3.50 (sept,  $J = 6.7$  Hz, 1H, CH-ipa), 4.16 (b.s., 2H,  $\text{NH}_2$ ), 7.36 (dd,  $J = 6.6, 1.5$  Hz, 2H, CH-py), 7.83 (td,  $J = 7.7, 1.7$  Hz, 1H, CH-py), 8.81 (dd,  $J = 6.6, 1.8$  Hz, 2H, CH-py).

$trans\text{-[PtI}_2(\text{ma})(\text{py})]$  **2** (orange solid). Yield: 15%. Elemental analysis found, C, 13.20; H, 1.94; N, 5.03;  $\text{C}_8\text{H}_{14}\text{I}_2\text{N}_2\text{Pt}$  requires C, 12.89; H, 1.80; N, 5.01. NMR (acetone- $d_6$ ):  $\delta$  (1H): 2.57 (t,  $J = 6.5$  Hz, 3H,  $\text{CH}_3\text{-ma}$ ), 4.20 (b.s., 2H,  $\text{NH}_2$ ), 7.40 (dd,  $J = 7.1, 1.51$  Hz, 2H, CH-py), 7.88 (td,  $J = 7.1, 1.9$  Hz, 1H, CH-py), 8.84 (dd,  $J = 6.6, 1.84$  Hz, 2H, CH-py).

##### 4.2. Nuclear Magnetic Resonance Spectroscopy

1D  $^1\text{H}$  NMR spectra were recorded on a 300 MHz Bruker Advance III HD (Bruker, Rivas-Vaciamadrid, Madrid, Spain) and 500 MHz DRX spectrometers (Bruker, Rivas-Vaciamadrid, Madrid, Spain). Solutions were prepared in acetone- $d_6$  for the characterization spectra and in a mixture of acetone- $d_6$  and  $\text{D}_2\text{O}$  in a ratio 2:1 for the interaction studies with the 5'-GMP and MeIm with a final concentration of  $[\text{Pt}] = 6.5$  mM.  $^1\text{H}$  chemical shifts were internally referenced to sodium 3-(trimethylsilyl)propionate (TSP).

##### 4.3. Irradiation

The light source used in the photoactivation experiments was a Photoreactor LZC-ICH2 from Luzchem (Ottawa, ON, Canada) fitted with UVA lamps (2 mW/cm $^2$ ,  $\lambda = 365$  nm). The temperature in



the light chamber during irradiation was kept at 37 °C and the sample preparation was performed as describe in the Section 4.2.

#### 4.4. X-ray Diffraction

The structural features of the new complexes **1** and **2** were unambiguously proven by X-ray diffraction. Data collection was performed on a Bruker Kappa Apex II (X8 APEX, Bruker, Rivas-Vaciamadrid, Madrid, Spain) area detector X-ray diffractometer using a graphite-monochromated Mo radiation. Crystal data and the structure refinement parameters are listed in Table S1. CCDC 913250 (complex **1**) and 913249 (complex **2**) contains the supplementary crystallographic data for this paper. These data can be obtained free of charge via <http://www.ccdc.cam.ac.uk/conts/retrieving.html> (or from the CCDC, 12 Union Road, Cambridge CB2 1EZ, UK; Fax: +44 1223 336033; E-mail: deposit@ccdc.cam.ac.uk).

#### 4.5. Cytotoxicity

SAOS-2 human osteosarcoma, A375 melanoma, T-47D breast cancer, SF-268 glioblastoma, NCI-H460 lung cancer cell lines were purchased from ATCC (Barcelona, Spain). Colorectal carcinoma cell lines HCT116 and matched p53-deficient HCT116 (−/−) were a kind gift of Bert Vogelstein (John-Hopkins University, Baltimore, MD, USA). These cell lines were cultured with DMEN (A375 and NCI-H460) or RPMI (HCT116) (Sigma, Madrid, Spain) with 10% fetal bovine serum, 2 mM L-glutamine, 100 U/mL penicillin and 100 µg/mL streptomycin in humidified air with 5% CO<sub>2</sub> at 37 °C.

The cytotoxicity was performed in Dr. Amancio Carnero's laboratory, following our published methodology, which is fully described in reference [6]. The compounds were dissolved in DMSO, diluted with PBS phosphate buffered saline to reach 10 mM solutions.

#### 4.6. DFT Calculations

All calculations on complexes **1** and **2** and their 9-EtG adducts were performed with the Gaussian 09 (G09) program [25] employing the DFT and TD-DFT [26,27] methods. Basis sets, ECPs for Pt and I and functionals were benchmarked (not shown) and the best combination in terms of performance and computational demand was the PBE1PBE:LANL08/6-31G\*\* [28] for geometry optimization and CAM-B3LYP/LANL08/6-31G\*\* [29] for electronic transition calculations (see below). The PCM solvent model [30] was adopted in all DFT and TD-DFT calculations with water as solvent. The nature of all stationary points was confirmed by normal mode analysis.

Thirty-two singlet excited states with the corresponding oscillator strengths were determined for the complexes at the ground-state geometry by TD-DFT. Theoretical UV-Vis spectra were obtained using GAUSSSUM 2.2 [31].

Molecular graphics images were produced using the UCSF Chimera package from the Resource for Biocomputing, Visualization, and Informatics at the University of California, San Francisco (supported by NIH P41 RR001081) [32].

## 5. Conclusions

We have presented two new diiodido complexes with aliphatic amines (ipa, **1** and ma, **2**) in *trans* to a pyridine ligand. Although the cytotoxicity of the complexes was not as encouraging as cisplatin and other similar compounds, their reactivity in the presence of UVA light and upon binding to model biological molecules revealed a new and interesting profile. We observed that irradiation at 365 nm enhances the DNA adduct formation at early stages (up to 1 h). Our photoactivation experiments suggest that longer irradiation times produce the release of the pyridine ligand and the subsequent generation of species that have previously proved to be active and interact with biomolecular targets.

Since this is the first time that we have observed the release of the spectator ligand in *trans*-type complexes, these results suggest that the aromatic nature of the amine ligand could play an important

role in the photochemistry of *trans* diiodido platinum complexes. We have identified two potential photoactivable compounds that showed two different photoactivation pathways.

**Supplementary Materials:** The following are available online at <http://www.mdpi.com/2304-6740/6/4/127/s1>, Cif and cifchecked files. Table S1. Crystal Data for complex 1 and 2; Figure S1. Progress of the reaction between complex 1 and 5'-GMP at 37 °C monitored by <sup>1</sup>H NMR (acetone-*d*<sub>6</sub> and D<sub>2</sub>O in a ratio 2:1) showing changes in the aromatic area and showing above the <sup>1</sup>H NMR (acetone-*d*<sub>6</sub> and D<sub>2</sub>O in a ratio 2:1) of non coordinated 5'-GMP and pyridine. Figure S2. Progress of the reaction between complex 2 and 5'-GMP at 37 °C monitored by <sup>1</sup>H NMR showing changes in the aromatic area. Table S2a. Selected bond distances (Å) for complexes 1 and 2 optimized with the DFT method at the PBE1PBE:LANL08/6-31G\*\* level using the PCM solvent (water) model. Table S2b. Selected bond distances (Å) for complex 2 optimized with the DFT method at the PBE1PBE:ECP/6-31G\*\* level using different ECPs for the Pt atom and the PCM solvent (water) model. Table S2c. Selected bond distances (Å) for complex 2 optimized with the DFT method at the PBE1PBE:LANL08/BS level using different basis sets (BS) for the non-Pt atoms and the PCM solvent (water) model. Table S2d. Selected bond distances (Å) for complex 2 optimized with the DFT method using different functionals, the LANL08/6-31G\*\* ECP/basis set and the PCM solvent (water) model. Table S3. Experimental and theoretical absorption spectra for complexes 1 and 2 in water at the CAM-B3LYP/LANL08/6-31G\*\* level. Table S4. Selected TD-DFT singlet-singlet transitions and corresponding electron difference density maps (EDDMs) for complexes 1 and 2 in water at the CAM-B3LYP/LANL08/6-31G\*\* level. Table S5. Experimental and theoretical absorption spectra for mono and bis 9-EtG adducts (complexes 3 to 6) of complexes 1 and 2 in water at the CAM-B3LYP/LANL08/6-31G\*\* level. Table S6. Selected TDDFT singlet-singlet transitions and corresponding electron difference density maps (EDDMs) for mono and bis 9-EtG adducts of complexes 1 and 2 in water at the CAM-B3LYP/LANL08/6-31G\*\* level. In the EDMs gray indicates a decrease in electron density, while blue-gray indicates an increase. Table S7. Selected frontier molecular orbitals for complexes 3 to 6. Table S8. Selected bond distances (Å) for the mono and bis 9-EtG adducts of complexes 1 and 2 optimized with the DFT method at the PBE1PBE:LANL08/6-31G\*\* level using the PCM solvent (water) model.

**Author Contributions:** Conceptualization: L.C. and A.G.Q.; Software, L.S.; Validation: L.C.; A.C., L.S., A.G.Q and A.I.M.; Formal Analysis and Data Curation: A.G.Q., A.I.M., L.S., A.C.; Investigation: L.C., T.P, A.G.Q., A.C., L.S., and A.I.M.; Resources: A.G.Q, A.C., L.S.; Writing—Original Draft Preparation: A.G.Q.; Writing—Review & Editing, A.G.Q., A.I.M., L.S., L.C.; Visualization: A.G.Q. and L.C.; Supervision, A.G.Q. and A.I.M.; Project Administration: A.G.Q.; Funding Acquisition: A.G.Q.

**Funding:** This research was funded by MINECO grant number CTQ-2015-68779R.

**Acknowledgments:** The MetDrugs network is acknowledged for providing opportunities for discussion.

**Conflicts of Interest:** The authors declare no conflict of interest.

## References

1. Johnstone, T.C.; Suntharalingam, K.; Lippard, S.J. The Next Generation of Platinum Drugs: Targeted Pt(II) Agents, Nanoparticle Delivery, and Pt(IV) Prodrugs. *Chem. Rev.* **2016**, *116*, 3436–3486. [[CrossRef](#)] [[PubMed](#)]
2. Medrano, A.; Dennis, S.M.; Alvarez-Valdes, A.; Perles, J.; McGregor Mason, T.; Quiroga, A.G. Synthesis, cytotoxicity, DNA interaction and cell cycle studies of *trans*-diiodophosphine Pt(II) complexes. *Dalton Trans.* **2015**, *44*, 3557–3562. [[CrossRef](#)] [[PubMed](#)]
3. Quiroga, A.G. Understanding *trans* platinum complexes as potential antitumor drugs beyond targeting DNA. *J. Inorg. Biochem.* **2012**, *114*, 106–112. [[CrossRef](#)] [[PubMed](#)]
4. Messori, L.; Casini, A.; Gabbiani, C.; Michelucci, E.; Cubo, L.; Rios-Luci, C.; Padron, J.M.; Navarro-Ranninger, C.; Quiroga, A.G. Cytotoxic Profile and Peculiar Reactivity with Biomolecules of a Novel "Rule-Breaker" Iodidoplatinum(II) Complex. *ACS Med. Chem. Lett.* **2010**, *1*, 381–385. [[CrossRef](#)] [[PubMed](#)]
5. Messori, L.; Cubo, L.; Gabbiani, C.; Alvarez-Valdes, A.; Michelucci, E.; Pieraccini, G.; Rios-Luci, C.; Leon, L.G.; Padron, J.M.; Navarro-Ranninger, C.; et al. Reactivity and Biological Properties of a Series of Cytotoxic Pt<sub>2</sub>(amine)<sub>2</sub> Complexes, Either *cis* or *trans* Configured. *Inorg. Chem.* **2012**, *51*, 1717–1726. [[CrossRef](#)] [[PubMed](#)]
6. Parro, T.; Medrano, M.A.; Cubo, L.; Munoz-Galvan, S.; Carnero, A.; Navarro-Ranninger, C.; Quiroga, A.G. The second generation of iodido complexes: *trans*-[Pt<sub>2</sub>(amine)(amine')] bearing different aliphatic amines. *J. Inorg. Biochem.* **2013**, *127*, 182–187. [[CrossRef](#)] [[PubMed](#)]
7. Starha, P.; Vanco, J.; Travnicek, Z.; Hosek, J.; Klusakova, J.; Dvorak, Z. Platinum(II) Iodido Complexes of 7-Azaindoles with Significant Antiproliferative Effects: An Old Story Revisited with Unexpected Outcomes. *PLoS ONE* **2016**, *11*, e0165062. [[CrossRef](#)]

8. Cubo, L.; Pizarro, A.M.; Quiroga, A.G.; Salassa, L.; Navarro-Ranninger, C.; Sadler, P.J. Photoactivation of *trans* diamine platinum complexes in aqueous solution and effect on reactivity towards nucleotides. *J. Inorg. Biochem.* **2010**, *104*, 909–918. [[CrossRef](#)]
9. Presa, A.; Brissos, R.F.; Caballero, A.B.; Borilovic, I.; Korrodi-Gregório, L.; Pérez-Tomás, R.; Roubeau, O.; Gamez, P. Photoswitching the Cytotoxic Properties of Platinum(II) Compounds. *Angew. Chem. Int. Ed.* **2014**, *54*, 4561–4565. [[CrossRef](#)]
10. Quental, L.; Raposinho, P.; Mendes, F.; Santos, I.; Navarro-Ranninger, C.; Alvarez-Valdes, A.; Huang, H.; Chao, H.; Rubbiani, R.; Gasser, G.; et al. Combining imaging and anticancer properties with new heterobimetallic Pt(II)/M(I) (M = Re, <sup>99</sup>mTc) complexes. *Dalton Trans.* **2017**, *46*, 14523–14536. [[CrossRef](#)]
11. Frei, A.; Rubbiani, R.; Tubafard, S.; Blacque, O.; Anstaett, P.; Felgenträger, A.; Maisch, T.; Spiccia, L.; Gasser, G. Synthesis, Characterization, and Biological Evaluation of New Ru(II) Polypyridyl Photosensitizers for Photodynamic Therapy. *J. Med. Chem.* **2014**, *57*, 7280–7292. [[CrossRef](#)] [[PubMed](#)]
12. Navas, F.; Perfahl, S.; Garino, C.; Salassa, L.; Novakova, O.; Navarro-Ranninger, C.; Bednarski, P.J.; Malina, J.; Quiroga, A.N.G. Increasing DNA reactivity and in vitro antitumor activity of *trans* diiodido Pt(II) complexes with UVA light. *J. Inorg. Biochem.* **2015**, *153*, 211–218. [[CrossRef](#)] [[PubMed](#)]
13. Aris, S.M.; Farrell, N.P. Towards Antitumor Active *trans*-Platinum Compounds. *Eur. J. Inorg. Chem.* **2009**, *2009*, 1293–1302. [[CrossRef](#)]
14. Farrell, N.P. Multi-platinum anti-cancer agents. Substitution-inert compounds for tumor selectivity and new targets. *Chem. Soc. Rev.* **2015**, *44*, 8773–8785. [[CrossRef](#)] [[PubMed](#)]
15. Brabec, V. DNA Modifications by antitumor platinum and ruthenium compounds: Their recognition and repair. In *Progress in Nucleic Acid Research and Molecular Biology*; Academic Press: New York, NY, USA, 2002; Volume 71, pp. 1–68.
16. Mellish, K.J.; Qu, Y.; Scarsdale, N.; Farrell, N. Effect of Geometric Isomerism in Dinuclear Platinum Antitumour Complexes on the Rate of Formation and Structure of Intrastrand Adducts with Oligonucleotides. *Nucleic Acids Res.* **1997**, *25*, 1265–1271. [[CrossRef](#)] [[PubMed](#)]
17. Zhao, Y.; Woods, J.A.; Farrer, N.J.; Robinson, K.S.; Pracharova, J.; Kasparikova, J.; Novakova, O.; Li, H.; Salassa, L.; Pizarro, A.M.; et al. Diazido Mixed-Amine Platinum(IV) Anticancer Complexes Activatable by Visible-Light Form Novel DNA Adducts. *Chem. A Eur. J.* **2013**, *19*, 9578–9591. [[CrossRef](#)] [[PubMed](#)]
18. Velders, A.H.; Quiroga, A.G.; Haasnoot, J.G.; Reedijk, J. Orientation- and Temperature-Dependent Rotational Behavior of Imidazole Ligands (L) in  $\beta$ -[Ru(azpy)<sub>2</sub>(L)<sub>2</sub>](PF<sub>6</sub>)<sub>2</sub> Complexes. *Eur. J. Inorg. Chem.* **2003**, *2003*, 713–719. [[CrossRef](#)]
19. Perez, J.M.; Montero, E.I.; Gonzalez, A.M.; Solans, X.; Font-Bardia, M.; Fuertes, M.A.; Alonso, C.; Navarro-Ranninger, C. X-ray Structure of Cytotoxic *trans*-[PtCl<sub>2</sub>(dimethylamine)(isopropylamine)]: Interstrand Cross-Link Efficiency, DNA Sequence Specificity, and Inhibition of the B–Z Transition. *J. Med. Chem.* **2000**, *43*, 2411–2418. [[CrossRef](#)]
20. Rochon, F.D.; Buculei, V. Multinuclear NMR study and crystal structures of complexes of the types *cis*- and *trans*-Pt(amine)<sub>2</sub>I<sub>2</sub>. *Inorg. Chim. Acta* **2004**, *357*, 2218–2230. [[CrossRef](#)]
21. Thiele, G.; Wagner, D. Über die Reaktion von Platiniodiden mit Pyridin und über die Molekül- und Kristallstruktur von *trans*-Diiodobis(pyridin)platin(II). *Chem. Ber.* **1978**, *111*, 3162–3170. [[CrossRef](#)]
22. Berger, I.; Nazarov, A.A.; Hartinger, C.G.; Groessl, M.; Valiahdi, S.-M.; Jakupec, M.A.; Keppler, B.K. A glucose derivative as natural alternative to the cyclohexane-1,2-diamine ligand in the anticancer drug oxaliplatin? *ChemMedChem* **2007**, *2*, 505–514. [[CrossRef](#)] [[PubMed](#)]
23. Tessier, C.; Rochon, F.D. Multinuclear NMR study and crystal structures of complexes of the types *cis*- and *trans*-Pt(Ŷpy)<sub>2</sub>X<sub>2</sub>, where Ŷpy=pyridine derivative and X=Cl and I. *Inorg. Chim. Acta* **1999**, *295*, 25–38. [[CrossRef](#)]
24. Rochon, F.D.; Tessier, C. Pt(II) compounds with sulfoxide ligands and crystal structures of complexes of the types I(R<sub>2</sub>SO)Pt(Ī<sup>1</sup>/<sub>4</sub>-I)<sub>2</sub>Pt(R<sub>2</sub>SO)I and *trans*-Pt(R<sub>2</sub>SO)(L)X<sub>2</sub> (L = amine, pyridine and pyrimidine). *Inorg. Chim. Acta* **2008**, *361*, 2591–2600. [[CrossRef](#)]
25. Frisch, M.J.; Schlegel, G.E.; Scuseria, M.A.; Robb, J.R.; Cheeseman, G.; Scalmani, V.; Barone, B.; Mennucci, G.A.; Petersson, H.; Nakatsuji, M.; et al. *Gaussian 09, Revision B.01*; Gaussian, Inc.: England, UK, 2009.
26. Stratmann, R.E.; Gustavo, E.S.; Michael, J.F. An efficient implementation of time-dependent density-functional theory for the calculation of excitation energies of large molecules. *J. Chem. Phys.* **1998**, *109*, 8218–8224. [[CrossRef](#)]

27. Mark, E.C.; Christine, J.; Kim, C.C.; Dennis, R.S. Molecular excitation energies to high-lying bound states from time-dependent density-functional response theory: Characterization and correction of the time-dependent local density approximation ionization threshold. *J. Chem. Phys.* **1998**, *108*, 4439–4449. [[CrossRef](#)]
28. Perdew, J.P.; Burke, K.; Ernzerhof, M. Generalized Gradient Approximation Made Simple. *Phys. Rev. Lett.* **1996**, *77*, 3865–3868. [[CrossRef](#)] [[PubMed](#)]
29. Yanai, T.; Tew, D.P.; Handy, N.C. A new hybrid exchange-correlation functional using the Coulomb-attenuating method (CAM-B3LYP). *Chem. Phys. Lett.* **2004**, *393*, 51–57. [[CrossRef](#)]
30. Miertu, S.; Scrocco, E.; Tomasi, J. Electrostatic interaction of a solute with a continuum. A direct utilization of AB initio molecular potentials for the prevision of solvent effects. *Chem. Phys.* **1981**, *55*, 117–129. [[CrossRef](#)]
31. O’Boyle, N.M.; Tenderholt, A.L.; Langner, K.M. cclib: A library for package-independent computational chemistry algorithms. *J. Comput. Chem.* **2008**, *29*, 839–845. [[CrossRef](#)] [[PubMed](#)]
32. Pettersen, E.F.; Goddard, T.D.; Huang, C.C.; Couch, G.S.; Greenblatt, D.M.; Meng, E.C.; Ferrin, T.E. UCSF ChimeraA visualization system for exploratory research and analysis. *J. Comput. Chem.* **2004**, *25*, 1605–1612. [[CrossRef](#)]



© 2018 by the authors. Licensee MDPI, Basel, Switzerland. This article is an open access article distributed under the terms and conditions of the Creative Commons Attribution (CC BY) license (<http://creativecommons.org/licenses/by/4.0/>).